AIMS Energy

AIMS Energy, 8(3): 455–473.
DOI: 10.3934/energy.2020.3.455
Received: 11 January 2020
Accepted: 01 June 2020
Published: 15 June 2020

http://www.aimspress.com/journal/energy

Research article

Solar assisted pyrolysis system for High-Density polyethylene plastic waste to fuel conversion

Aklilu T. Habtewold*, Demiss A. Ambie, and Wondwossen B. Eremed

School of Mechanical and Industrial Engineering, Addis Ababa Institute of Technology

* **Correspondence:** Email: aklilu.tesfaye@aait.edu.et; Tel: +251911036741.

Abstract: Plastic products are used almost in all our daily life activities due to their characteristics such as being inert, durability, flexibility, and versatility. More than 1 million tons of plastic wastes are generated daily in Ethiopia. Unless managed it properly plastic waste affects the environment immensely since they are durable and stable. Plastic wastes stay in the environment for a long time. In this paper, a solar-assisted pyrolysis system has been designed and tested for the generation of liquid fuel from High-Density Polyethylene plastic waste. Data were collected related to the solar energy potential of Addis Ababa city of Ethiopia and the amount of plastic waste generated daily. Proximate and ultimate analysis and heating value of waste were determined experimentally. The energy requirements of the pyrolysis system were determined and the sizing of the system was performed. The model is simulated using Matlab software and a mathematical model is applied to study the performance of the system. A 4 m diameter solar parabolic dish collector with a cylindrical-shaped reactor at the focal point and dual solar tracking system is used based on Addis Ababa weather data and the required energy for the endothermic pyrolysis. Based on the result, the conversion efficiency of the system is 72% by weight. The result also shows 1360 Kwh/m^2 of solar energy is required to produce 14.2 liters of liquid fuel from High-Density Polyethylene plastic waste. The heating value of the produced liquid fuel is 41.8 MJ/kg. Thus, by using a solar-assisted pyrolysis system a liquid fuel has been produced from plastic waste, income is generated from the selling of the produced liquid fuel, and the environmental impact of waste plastic is reduced.

Keywords: solar-assisted pyrolysis; High-Density Polyethylene; waste; fuel; heating value

1. Introduction

Plastic plays a significant role in our day-to-day activities. The demand for plastic is increasing though the waste management aspects of plastic are still not developed mainly in developing countries [1]. Plastic waste comprises mainly of low-density polyethylene, high-density polyethylene, polyethylene terephthalate, polypropylene, polystyrene, and polyvinyl chloride [2]. The natural degradation of plastic wastes needs more than 500 years and making it the most evident constituent of landfills [3].

In Ethiopia, more than 1 million tons of plastic waste is disposed of daily. Even though there are some initiatives of plastic recycling around urban areas [4,5], only 10 percent of the total plastic waste generated is collected. The most common types of polyethylene are low-density polyethylene and high-density polyethylene [6]. High-density polyethylene is the third-largest commodity plastic material in the world, after polyvinyl chloride and polypropylene in terms of volume [7].

Pyrolysis, a thermal conversion process, is unarguably one of the most promising technologies for fuel production from different waste plastics [8–11]. Pyrolysis of waste plastic was conducted in the absence of oxygen at a temperature between 350 and 900 ℃ [12]. The pyrolysis process of plastic waste results in the formation of a carbonized char (solid residues) and a volatile fraction that may be separated into condensable hydrocarbon oil and a non- condensable high calorific value gas. The proportion of each fraction and their composition depends primarily on the nature of the plastic waste and the process conditions [11–13]. The major factors that affect the pyrolysis products are among others, conversion technology, temperature, and pressure.

Even though several researchers tested pyrolysis for producing liquid fuel from plastic waste [10,14–16], pyrolysis units should be designed with a clear business model in mind [8]. Improving the efficiency of the system i.e., making it economical and environmentally friendly must be a priority. Besides, pyrolysis is a process that requires energy supplied from external sources either by the combustion of fuel or electrical energy [17–19]. This heat comes with a price. Therefore, the issues of the required energy can be solved by using a solar heating system. To this effect, Ethiopia has a huge solar energy potential that is sufficient for this kind of system.

Solar energy has been using for various thermal conversion processes based upon the absorption of solar radiation in concentrated form by lenses or mirrors using a black absorbing surface. Various studies have been done on the solar thermal conversion process: gasification of plastic waste [20–22], pyrolysis of plastic waste [23,24]. Plastic waste is also used directly as fuel in fuel cell and electrolyzer by applying an electrochemical cell to the reaction system to produce electricity or useful chemicals from plastic raw materials [25].

So addressing the challenge of plastic waste problem plays a significant role in protecting the environment. The liquid fuel, generated from plastic waste can be used for highly efficient applications i.e., for the internal combustion engine, generator and others.

In this paper, a detailed analysis has been conducted on the solar-assisted pyrolysis system for high-density polyethylene plastic waste for the production of fuel. Solar radiation data of Addis Ababa city was taken, based on which, the input sample of the system; sizing has been determined using mass and energy balance. Moreover, according to the sizing information of the design, the solar-assisted pyrolysis system has been manufactured and tested. Proximate and ultimate analysis and heating value of the produced fuel have been performed. This paper aims to identify the fuel production favorability and mechanism using solar energy and other heat sources from high-density polyethylene plastic waste in Addis Ababa.

2. Material and methods

Prior to the modeling of the solar-assisted pyrolysis system, the determination of waste generation rate, type, and location weather data are collected. Modeling of the system been done using mathematical equations. The outputs from this are used for Matlab simulation.

2.1. HDPE plastic waste generation rate

The plastic waste generation rate in Addis Ababa is about 5.2% of the total solid waste generation. This rate increases with the economic growth and development of the country. There are more than 500 plastic companies, registered with the Ethiopian Ministry of Trade and Industry.

2.2. High-density polyethylene (HDPE) plastic waste characterization

Thermoplastic is a polymer made from ethylene monomer and it has a thermal conductivity of 0.44 W/m K, melting point of 134 ℃, as well as latent heat of fusion of 178.6 kJ/kg, and a maximum temperature of decomposition of 475 ℃. It has the number two as its resin code.

2.2.1. Proximate and ultimate analysis and heating value

The proximate analysis of HDPE samples such as moisture content, ash content, volatile matter, and fixed carbon content was determined by standard procedures of American Society for Testing and Material (ASTM) method number D1762-4 (ASTM method, D-1762-84). The ultimate analysis was also conducted to directly determine the carbon, hydrogen, nitrogen and Sulphur contents of HDPE samples by using EA 1112 Flash CHNS/O analyzer model with carrier gas flow rate of 120 ml/min, reference flow rate 100 ml/min, oxygen flow rate of 250 ml/min; furnace temperature of 900 ℃ and oven temperature of 75 ℃. The sample was set in duplicate and the average values are to be taken as shown in Table 1. HDPE sample is weighted and placed in a digital bomb calorimeter for calorific value or heating value determination. The measured lower heating value of HDPE is 41.8 MJ/kg.

Table 1. Proximate and ultimate analysis, heating value, and density of HDPE Plastic Waste.

Parameters	HDPE waste samples
Moisture content (wt. %)	0.15
Ash content (wt. %)	3.73
Volatile content (wt. %)	92.04
Fixed carbon (wt. %)	4.08
Total (wt. %)	100
Lower heating value (MJ/kg)	41.8
Pure Density	0.87
C	81.69
H	13.72
O	3.75
N	0.58
S	0.26
Total (%)	100

2.3. The working principle of the pyrolysis system

There are two reactors in the plant the solar rector and the screw reactor. The solar reactor solar energy heating system and the screw reactor heated by the combustion of fuel or biomass available.

The main reason to incorporate the second screw reactor is to further decompose uniformly the molten plastic that leaves the solar reactor as semi-fluid, which is about 30 to 50 percent of the intake feedstock at solar reactor intake. As can be seen from Figure 3 the reactor has a screw to mix the feedstock for good heat transfer inside the reactor. There are also other advantages to mention one for continuous fuel production capacity during low irradiation time in the daytime and no radiation at the nighttime.

2.3.1. Plastic waste pretreatment

Plastic waste must be pretreated to improve the quantity and quality of product oil. This pretreatment includes sorting according to its type, washing, drying, and crushing into a small size of about 3–5 mm as shown in Figure 1.

Figure 1. Pretreated HDPE for the pyrolysis system.

2.3.2. Feeding system for solar reactor

The feeding system has four main parts. The handle, the moving channel, the material container, and the slid container supports. The feeding mechanism operates manually as shown in Figure 2. The feeding system can be detached and move the opposite side of the dish by removing the pin connection shown at Detail c in Figure 2 to use the feeding system for opposite inclination in the afternoon.

There are two ball bearing at the bottom of the container as a wheel to drive the feeding container through the guide channel.

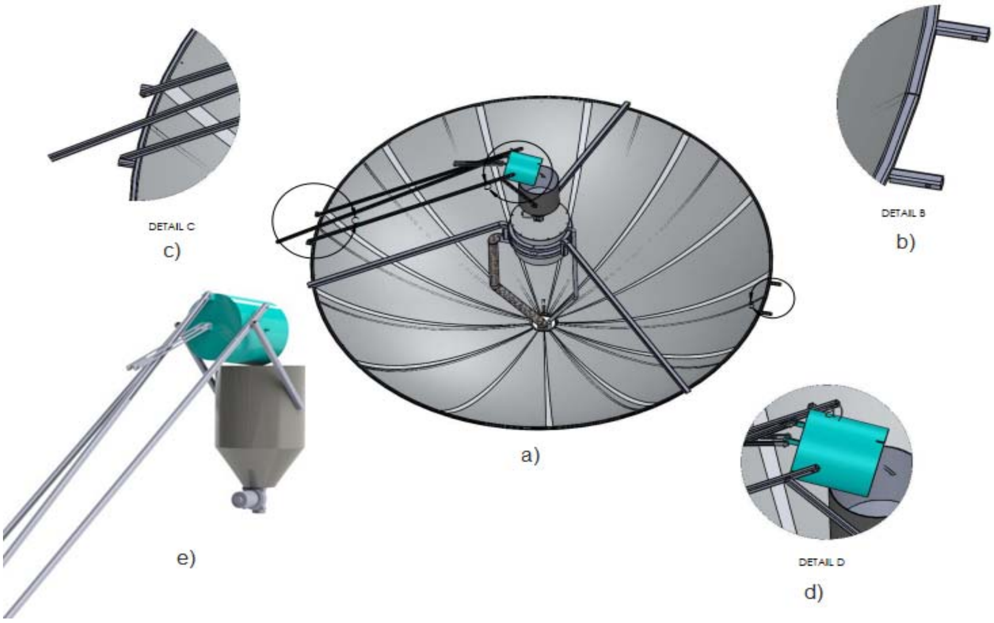

Figure 2. a) Feedstock Feeding System with the Reactor; b) Dish Extension with Hole for Feeding System Connections; c) Feeder Handle; d) Feedstock Feeding System; e) Rendered 3D Feeding System.

2.3.3. Overall Pyrolysis Plant working principle

The solar reactor and the biomass reactor must be purged using nitrogen gas to avoid any oxygen presence. Then 11 kg of crushed plastic waste was added at the top of the solar reactor intake (59) using the feeding mechanism mentioned above (5).

Then heating the solar reactor (61) by closing the intake valve (182) up to 550 ℃ for 30 minutes with a heating rate of 17.5 ℃/min, by adjusting the solar collector (32) at the correct position as shown in Figure 3. Then set the solenoid valve (182) by adjusting it to pass 1 kg every 3 minutes since the addition of the feedstock every 30 minutes is required so that 1 kg of plastic waste will prevent the passage of oxygen through the valve during the opening at the end of each intake. There will be three products from the process at the end; the pyrolysis gases through a ½-inch pipe (51), liquid, and solid char passing through a 2.5-inch metal hose (221).

The vapor will pass to the cyclone together with the vapor from the screw reactor exhaust (54) to drop the solid char where some of the heavy pyrolysis oil will be condensed at the bottom container (12). Since it has a large surface area for heat exchange with the environment i.e. with much less than the vapor temperature then the relatively purified vapor goes to the condenser to be condensed where the non-condensable gas will be collected in the syngas tanker (3) to be used for the combustion chamber later on. The condensed liquid will be drawn using an oil pump (103) store at the oil tank (25) for further use.

The liquid product and the char will leave the solar reactor at the bottom exit (221) directly passing to the second reactor (61), and heated by both the burning of the collected syngas from syngas tank and the biomass at the combustion chamber (2), for further thermal decomposition within a controlled environment. Similar to the solar reactor the second reactor has also two exits: the upper and bottom. Through upper exit, the vapor leaves (54) and mix with the vapor from the solar reactor and through the bottom exit the char finally mixes with the biomass in the combustion chamber (2) which is fired by a mixture of forced air from the blower (13), and syngas and biomass.

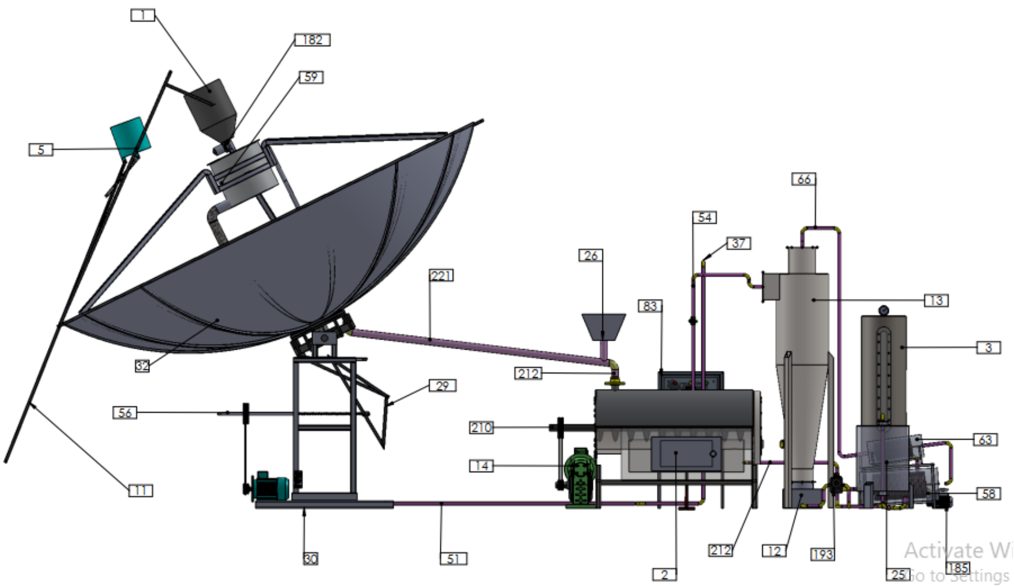

Figure 3. Solar assisted pyrolysis plant layout.

The dual tracking system includes both manual operations by using the handle (56) and by an automated system integrating motor and Ac drive rotation controller (4).

Temperature, pressure, and flow rate measurements are made using a centralized board and k type thermocouple (83), pressure gauges (212), and gas and liquid flow meter (83) respectively.

2.4. Modeling of the reactors for the pyrolysis plant

There are two reactors: as can be seen from Figure 4. The first reactor, installed at the solar collector and operated solely by solar irradiation concentrated at the bottom part of the reactor. This reactor vaporizes almost half of the HDPE feedstock at minimum capacity and above 70 percent at maximum capacity and passing the rest to further vaporize at the second reactor, a screw reactor, for which a combustion chamber to burn biomass for endothermic thermolysis process.

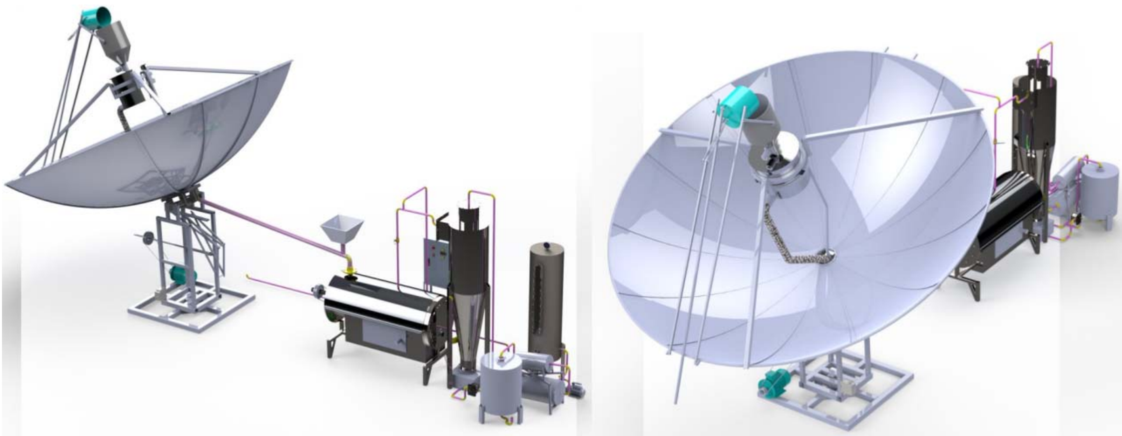

Figure 4. Schematic drawing of solar-assisted pyrolysis system.

2.4.1. Solar irradiation

The solar irradiation data from 2012 up to 2016 for the city was taken and direct irradiation of the five years average value was used for the sizing. It is recorded between 15 minutes of gaps to increase the accuracy of determining the monthly average value. The data is from the Ethiopian National Meteorological Services Agency (NMSA) which is a marlin for installing, collecting, and archiving of meteorological and climatological data. After the determination of the average direct normal irradiation, sizing of the dish is performed with the minimum monthly average value in June i.e., 545.664 W/m^2.

2.4.2. Sizing of solar collector

The parabolic dish collector is selected due to its high concentration ratio, low maintenance requirement, and easy for installation and favorability for small-scale applications. Sizing of the parabolic dish mainly depends on the required energy and solar radiation of the area where used. The solar reactor installed requires 4.75 kW power to decompose a waste high-density polyethylene at a mass flow rate of 20 kg/hr (0.0056 kg/s) while the implementation place of solar irradiant stands at 545.664 W/m^2 minimum monthly average value in June. Using these values, a 4 m diameter parabolic dish has been designed where aluminum was selected for the reflective material with a reflectivity of 0.92.

2.4.3. The energy balance for the system

The energy required to change the waste HDPE into the pyrolysis products (Syngas, pyrolysis oil and char) can be calculated using the definition of the specific heat definition and i.e., the energy needed to change 1 kg of HDPE by 1 °C which is called specific heat and 1.72 kJ/kg °C was taken as an average value. The maximum temperature for the decomposition of HDPE is 550 °C while a feedstock HDPE with initial temperature stands at 52 °C where the required energy for the decomposition of HDPE can be calculated using Eq 1:

$$\dot{Q}_r = C_p \Delta T \dot{m} \qquad (1)$$

The incident solar energy entering the parabolic dish collector for Addis Ababa location can be determined from the beam solar irradiance of Addis Ababa at the decimal latitude and longitude coordinates 9.02497 and 38.74689 respectively can be given by Eq 2:

$$\dot{Q}_i = I_b \times A_{ap} \qquad (2)$$

$$A_{ap} = \frac{D_a^2 \pi}{4} \qquad (3)$$

The optical efficiency of the parabolic dish solar collector, defined as the ratio of energy reaching the receiver to that received by the collector is calculated by using Eq 4:

$$\eta_{opt} = \rho_c \tau_v \alpha s \cos\theta \qquad (4)$$

The total energy absorbed at the absorber, which is equal to the product of optical efficiency and the amount of energy collected from the sun at the given location can be obtained by Eq 5:

$$\dot{Q}_a = \eta_{opt} \times \dot{Q}_i \qquad (5)$$

Heat loss at the collector is the difference of the incident energy at the collector minus the absorbed energy at the absorber of the solar reactor as given by Eq 6:

$$\dot{Q}_{c,l} = \dot{Q}_i - \dot{Q}_a \qquad (6)$$

For the solar collector, the energy conversion process can be determined using the energy balance equation. For the useful energy, the output of the receiver equals the absorbed solar energy minus the total thermal losses from the receiver (solar reactor absorber). The useful energy can be computed using Eqs 7 and 8:

$$\dot{Q}_u = \dot{Q}_a - \dot{Q}_l \quad \text{...(7)}$$

$$\dot{Q}_u = \dot{m}C_p(T_{sr,out} - T_{sr,in}) \quad \text{...................................(8)}$$

Heat loss from the solar reactor absorber is determined by using Eq 9:

$$\dot{Q}_{l,sr} = A_{abs}U_{l,r}(T_{sr,av} - T_{am}) \quad \text{...............................(9)}$$

By applying the first law of thermodynamic energy balance equation on the solar reactor absorber space, the useful energy, is calculated by Eq 10:

$$\dot{Q}_u = \eta_{opt}I_bA_{ap} - A_{abs}U_{l,r}(T_{sr,av} - T_{am}) - \frac{\rho_{ab}V_{ab}C_{p,ab}dT_{ab}}{dt} \quad \text{..............(10)}$$

The value for overall heat transfer coefficient, $U_{l,r}$, using the convective and convective heat transfer coefficient is given by Eq 11:

$$U_{l,r} = \left[\frac{1}{h_r + h_c}\right]^{-1} \quad \text{.................... ....(11)}$$

The coefficient of radiation heat loss is given by Eq 12 [26]:

$$h_r = \sigma\varepsilon_{sr}\left(T_{sr}^{\;2} + T_{am}^{\;2}\right)\left(T_{sr} + T_{am}\right) \text{...............................(12)}$$

Moreover, the natural convection is determined from the Nusselt number correlation equation using Eq 13:

$$h_r = \frac{K_{air}}{D_v} \times Nu \quad \text{...(13)}$$

The Reynold number can be computed using the Eq 14:

$$\mathrm{Re} = \frac{V_{air} \times D_v}{\gamma_{air}} \quad \text{.......................................(14)}$$

Hence for Reynold number included between 0.1 and 1000, the Nusselt number is given by Eq 15:

$$Nu = 0.4 + 0.54\,\mathrm{Re}^{0.52} \quad \text{........ ....(15)}$$

The energy in with the waste HDPE is the energy contained by the feedstock entering the solar reactor at 20 kg/hr can be calculated, assuming a temperature difference of 30 for average 22 °C ambient temperature of the city since it is pretreated.

$$E_{fd} = \dot{m}C_p\Delta T \quad \text{..(16)}$$

The instantaneous thermal efficiency of the solar reactor can be defined as the ratio of heat gained at the solar reactor, Q_u, to the total incident solar energy, Q_i. This is calculated using Eq 17:

$$\eta_t = \frac{Q_u}{Q_i} \quad \text{......................................} (17)$$

2.4.4. Computational model

The temperature at the absorber of the solar reactor can be given as using the energy balance at the absorber, where the next time step is given using Eq 18:

$$T_{ab,i+1} = T_{ab,i} + \frac{\Delta t}{m \times C_{p_{ab}}} \left(I_{b,i} \times A_c \times \eta_{opt} - A_c \times U_{l,r,i} \times \left(T_{ab,i} - T_{amb} \right) \right) \quad \text{......} (18)$$

For the different temperature, there is a corresponding overall heat transfer coefficient determined by Eq 19:

$$U_{l,r,i} = \left[\frac{1}{h_{r,i} + h_c} \right]^{-1} \quad \text{......................................} (19)$$

However, radiative heat transfer constant is given by Eq 21:

$$h_{r,i} = \sigma \times \varepsilon \times \frac{\left(T_{ab,i}{}^4 - T_{amb}{}^4 \right)}{\left(T_{ab,i} - T_{amb} \right)} \quad \text{......................................} (20)$$

2.5. Model simulation

Before explaining the simulation of the proposed model in MATLAB software, it needs to be illustrated that there are two types of inputs, which are input parameters and input variables. The input parameters are the inputs that do not vary with the time and have thus fixed values which are given by Table 2. On the other hand, the input variables are varying with time; and they are required to observe and investigate their variability effect on optical properties and thermal performance of the parabolic dish solar heating system through Matlab simulation for proper optimization. The input parameters concerning geometric properties are the aperture area and depth of the parabolic dish solar collector i.e., internal and external diameters of the receiver and thickness of the receiver.

Table 2. Pyrolysis system model input and predetermined parameters [26].

Parameters	Symbols	Values	Unit
The reflectance of the collector	ρ_c	0.92	[-]
Collector of emittance	ε_c	0.5	[-]
Collector aperture diameter	D_a	4	[m]
Wind velocity	v_w	4	[m/s]
Aperture area	A_{ap}	12.57	[m^2]
Ambient temperature	T_{amb}	23	[°C]
Specific heat of HDPE	C_P	1.9	[kJ/kg.K]
Focal distance	f	1.2	[m]
Depth of diameter	d	0.833	[m]
Length of the parabolic segment	L	2.62	[m]
The surface area of a parabolic reflector	S	14.54	[m]
Receiver absorbance	α	0.85	[-]
The transmittance of glass envelope covering the receiver	τ_v	1	[-]
Slope error		3	[degree]
Specularity error		0.5	[degree]
The inner diameter of the receiver	d_{ri}	0.3302	[m]
The outer diameter of the receiver	d_{ro}	0.323	[m]
Solar reactor absorber area	A_{ab}	0.005024	[m^2]
The mass flow rate of HDPE for the solar reactor intake	$\dot{m}_{sr(in)}$	20	[kg/hr]
The mass flow rate of HDPE for the biomass reactor intake	$\dot{m}_{br(in)}$	10.4	[kg/hr]
The volume of HDPE in the solar reactor	V_{HDPE}	0.0265	[m^3]
Stefan-Boltzmann constant	σ	5.67×10^{-8}	[W m/K^4]
Kinematic viscosity air`	υ	$1.52 \times 10^{-}5$	$W/m^2.K^4$]
Velocity of air	V_a	4	[m/s]
Thermal conductivity of the receiver material	k		[W/m K]
Thermal conductivity of HDPE	K_{HDPE}	0.48	[W/m K]
Receiver shading factor	s	1	[-]

2.5.1. Flow chart for Matlab program

As the flow chart Figure 5 shows, the inputs to the program are the beam irradiance for the representative days of the year every 15-minutes as well as collector design parameters, and constants from the Table 2. For every 15-minute, the solar beam irradiance on the collector surface is computed and plotted against time. The absorber temperature the useful thermal energy and incident energy at the collector, are determined for every time step.

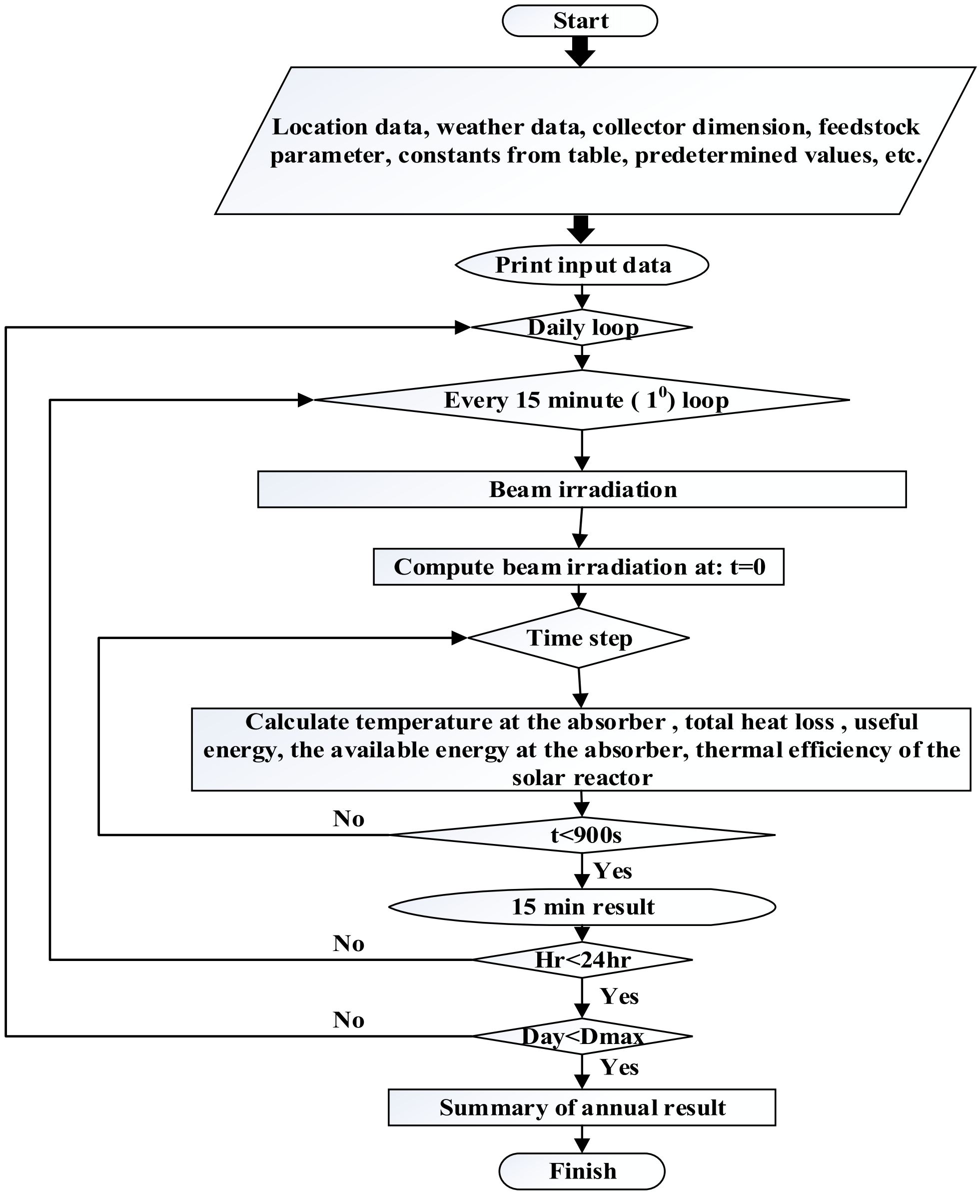

Figure 5. Flow chart of the model.

3. Results and discussion

According to the data from Addis Ababa Solid Waste Management Agency HDPE, solid waste is more available. Addis Ababa city selected for the implementation of the project because of the availability of plastic waste. The system uses a 4 m aperture area of parabolic dish collector wherein the simulated model, the lowest average solar irradiation intensity is about 545.664 W/m^2 in June and the highest of 891.12 W/m^2 in March. The temperature of the receiver from 450 ℃ to 1200 ℃ within the peak hours of the day (8:00 AM–5:00 PM).

3.1. Mass balance analysis for solar assisted pyrolysis system

The mass balance Sankey diagram for the solar pyrolysis given by Figure 6 HDPE plastic is feed into the pyrolysis reactor with a mass flow rate of 20 kg/hr. The 52 percent of the output by mass is pyrolysis gas whereas 48 percent by mass of the product become char and cake type solid, requiring further decomposition due to poor heat transfer between the crushed plastic waste.

The 48 percent char and cake type plastic waste goes to the screw (biomass) reactor together with fresh waste HDPE and generates an average of 72 percent of pyrolysis oil, 15 percent syngas, and the remaining into char.

Compared to the other pyrolysis plant which uses no solar energy for the heating process there is a reduction of more than half the energy cost of the system for the heating system at minimum irradiation and more than 70 percent for the maximum irradiation.

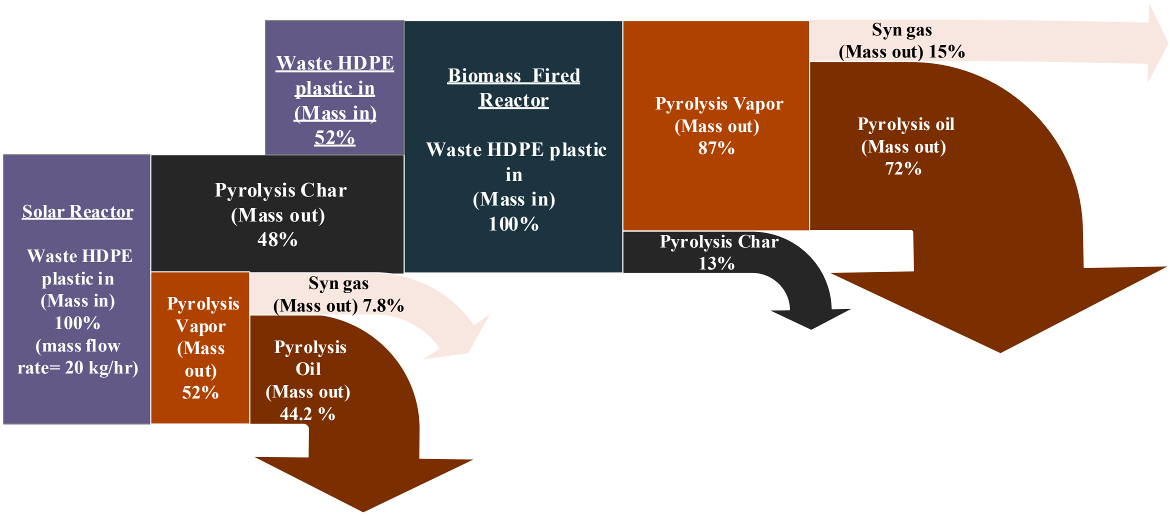

Figure 6. Mass Balance of the pyrolysis system.

The energy balance Sankey diagram for solar reactor shown by Figure 7 illustrates the total energy incident on the collector, heat loss at the collector, useful energy at the absorber, heat loss at the absorber, energy in with the feedstock, energy out with the pyrolysis vapor and solid, and energy stored within the reactor.

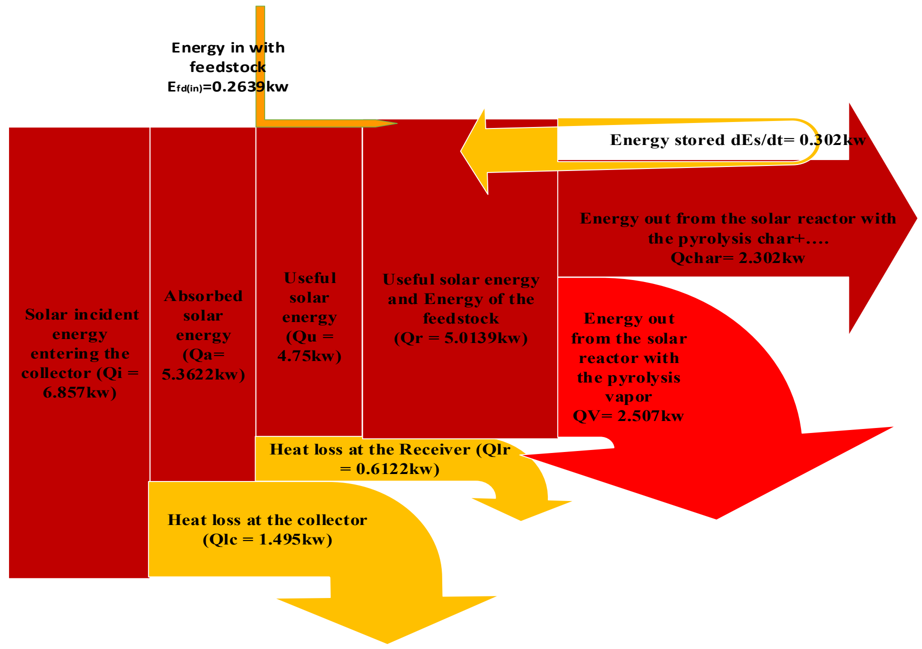

Figure 7. Energy balance for the solar reactor.

The energy balance Sankey diagram of a biomass reactor given by Figure 8**.** It shows the energy in from the solar reactor, loss through the pipe, the energy in from biomass combustor, heat loss at the combustor, useful energy at the absorber, heat loss at the reactor, energy in with the feedstock, energy out with the pyrolysis vapor and solid, and energy stored within the reactor.

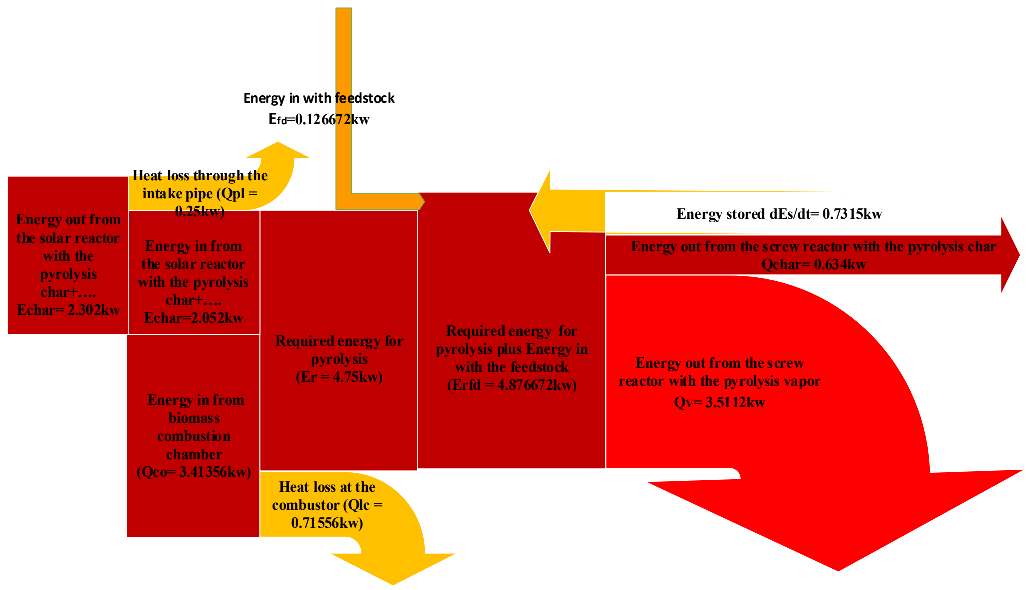

Figure 8. Energy balance for biomass screw reactor.

Summary of values from the mathematical modeling and Figure 7, and Figure 8 are given in Table 3 with the corresponding symbol, unit, and reference.

Table 3. Summary of the energy balance of the system for the instantaneous state.

Parameters	Symbols	Values	Unit	References
The energy required for pyrolysis	$\dot{E}_{re(sr)}$	4.75	[kW]	Eq 1
Incident solar energy at the collector	Q_i	6.857	[kW]	Eq 2
The optical efficiency of the collector	η_{opt}	0.782	[-]	Eq 4
Heat loss at the collector	Q_{lc}	1.495	[kW]	Eq 6
Absorbed solar energy at the receiver	Q_a	5.3622	[kW]	Eq 5
Heat loss at the solar reactor	Q_{lr}	0.6122	[kW]	Eq 9
Useful solar energy for solar reactor	Q_u	4.75	[kW]	Eq 7
The thermal efficiency of the solar reactor	η_{th}	0.693	[-]	Eq 17
The energy in with the feedstock for solar reactor	$\dot{E}_{fd(in)}$	0.2639	[kW]	Eq 16
Energy stored at solar reactor	$\dot{E}_{st}$	0.302	[kW]	Eq 1
Energy out with pyrolysis vapor	$Q_{v(out)}$	2.507	[kW]	Eq 16
Energy out with pyrolysis char and liquid	$Q_{char(out)}$	2.302	[kW]	Eq 16
Heat loss through the intake pipe	Q_{lp}	0.35	[kW]	Eq 1
The energy in from the solar reactor with the pyrolysis char	$Q_{char(in\_br)}$	1.952	[kW]	Eq 16
Energy in from biomass combustion chamber	Q_{co}	3.41356	[kW]	Eq 18
Heat loss at the combustor	Q_{lc}	0.71556	[kW]	Eq 1
Energy in with feedstock	$\dot{E}_{fd(br)}$	0.126672	[kW]	Eq 1
The required energy for the pyrolysis	$\dot{E}_{r(br)}$	4.75	[kW]	Eq 1
The required energy for pyrolysis plus Energy in with the feedstock	$\dot{E}_{rfd(br)}$	4.876672	[kW]	Eqs 1 and 10
Energy stored at the screw reactor	$\dot{E}_{st(br)}$	0.7315	[kW]	Eq 1
Energy out from the screw reactor with the pyrolysis char	$Q_{char(br)}$	0.634	[kW]	Eq 16
Energy out from the screw reactor with the pyrolysis vapor	$Q_{v(sr)}$	3.5112	[kW]	Eq 16

3.2. Transient thermal analysis

The average yearly solar beam irradiation for representative days of the months for 24 hrs period for 15-minute interval data has been shown by Figure 9. The maximum average direct solar irradiation is registered in March is 891.12 W/m^2 while the minimum average value for beam irradiation in June is 545.664 W/m^2.

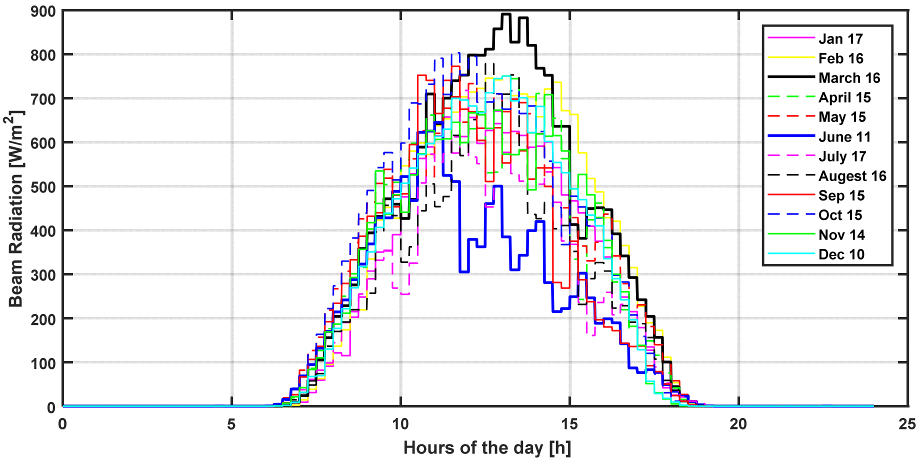

Figure 9. Average Solar Irradiation for the representative day of the month vs Hours of the day.

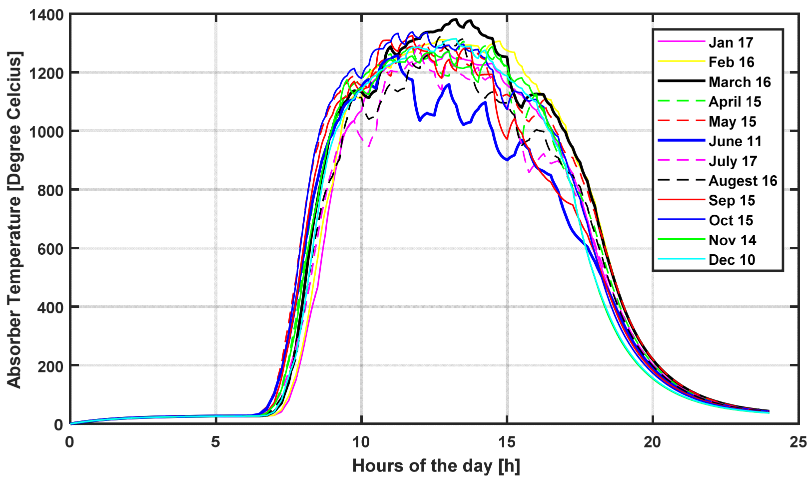

Figure 10. Reciever temperature for the representative day of the month vs Hours of the day.

The variable temperature at the receiver has been calculated using Eq 18. As can be seen from the Figure 10, the peak hours that the dish traps adequate temperature between 450 °C and 1300 °C for thermal decomposition of HDPE waste is 9 hours per day, from 8:00 am to 5:00 pm; so the required temperature can be attained throughout the year in between these hours.

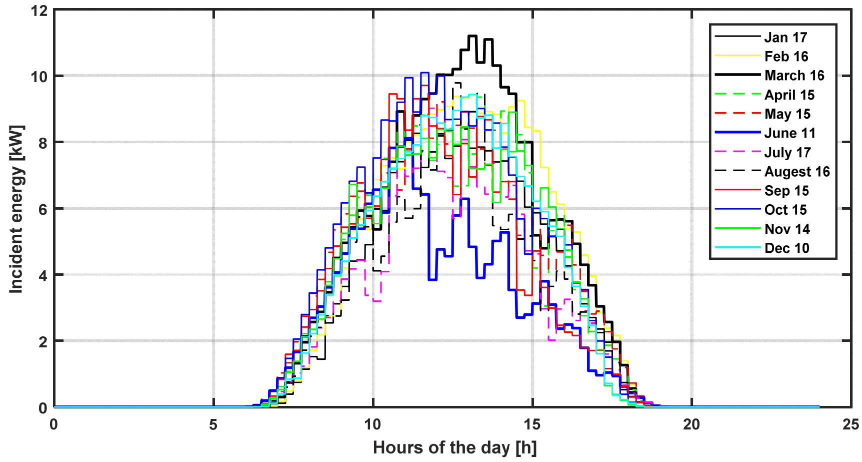

Figure 11. Five years average incident energy at the collector.

The incident energy at the collector, which is a product of the solar irradiant, reaching the surface and the collector area as can be seen in Figure 11 has an average maximum value in March within the peak hours of 7.21 kW and minimum in June of 5.2 kW.

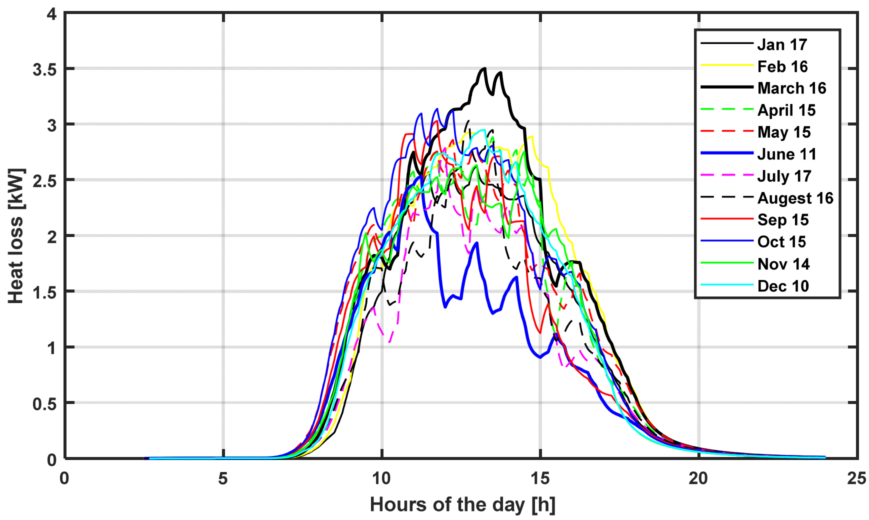

Figure 12. Five Years Average heat loss energy at the absorber of the solar reactor.

The heat loss at the absorber of the solar reactor as can be seen in Figure 12, has an average maximum value in March within the peak hours of 2.32 kW and minimum in June of 0.52 kW.

4. Conclusions

The results of this detailed study on the Solar-assisted Pyrolysis System for the Production of fuel from High-density Polyethylene Plastic Waste shows that the energy required for the pyrolysis system has been produced by using the available solar irradiation of Addis Ababa City. The system needs 4.75 kW of energy. By using a 4m diameter parabolic dish, it is possible to attain the required energy. Thus, the use of solar energy for the pyrolysis system decreases the extensive heat energy required to decompose the HDPE consumption of biomass by 48 percent at lowest irradiation in June with minimum average irradiant of 545.664 W/m^2 and 72 percent at highest irradiation registered in March with maximum irradiant of 891.12 w/m^2.

This system will substantially reduce the rising cost of fuel and electricity in the country. Apart from serving as an energy resource, it helps the efforts made to create a clean environment and removing toxic gaseous release from landfills and incineration. Comparatively, the solar energy heating system has low maintenance and running costs than the other heating system including the biomass combustor system. This results in the reduction of production cost, apart from supplying produced liquid fuel at low cost for the users. The research finding has identified how a small-scale fuel production system could be designed, manufactured, and made operational from waste plastic materials with renewable energy sources and low cost.

Acknowledgments

The authors acknowledge the financial support of the Vice President for Research and Technology Transfer Office of Addis Ababa University.

Conflict of interest

All authors declare no conflict of interest in this paper.

References

1. Commission, European (2011) Plastic waste : Ecological and human health impacts.
2. The American Chemistry Council (2015) 2015 Plastics-To-Fuel Project Developer's Guide. *Ocean Recovery Alliance*.
3. Barnes DKA, Galgani F, Thompson RC, et al. (2009) Accumulation and fragmentation of plastic debris in global environments. *Philos Trans R Soc B Biol Sci* 364: 1985–1998.
4. Asgedom AG, Desta MB (2012) The environmental impacts of the disposal of plastic ags and water bottles in Tigray, Northern Ethiopia. *Sacha J Environ Stud* 2: 81–94.
5. Negussie B, Mustefa J (2017) Environmental public health performance standards—Environmental health program Self-assessment instrument. (Version 2), *Pollution* 3: 147–156.
6. Sogancioglu M, Yel E, Ahmetli G (2017) Pyrolysis of waste high-density polyethylene (HDPE) and low-density polyethylene (LDPE) plastics and production of epoxy composites with their pyrolysis chars. *J Clean Prod* 165: 369–381.
7. Kumar S, Singh RK (2014) Pyrolysis kinetics of waste High-density polyethylene using thermogravimetric analysis. 6: 131–137.
8. Garcia-Perez M, Al E (2013) *Methods for Producing Biochar and Advanced Biofuels in Washington State. Part 3: Literature Review* 12: 125.
9. Safadi Y, Zeaiter J, Ahmad M (2013) Advanced modeling of high-density polyethylene pyrolysis. 5: 123–128.
10. Lombardi L, Carnevale E, Corti A (2015) A review of technologies and performances of thermal treatment systems for energy recovery from waste. *Waste Manage* 37: 26–44.

11. Panda AK, Singh RK (2013) Experimental optimization of process for the Thermo-catalytic degradation of waste polypropylene to liquid fuel. *Adv Energy Eng* 1.
12. Panda AK, Singh RK, Mishra DK (2010) Thermolysis of waste plastics to liquid fuel A suitable method for plastic waste management and manufacture of value-added products—A world prospective. 14: 233–248.
13. Panda AK, Murugan S, Singh RK (2016) Performance and emission characteristics of diesel fuel produced from waste plastic oil obtained by catalytic pyrolysis of waste polypropylene. *Energy Sources, Part A Recover. Util Environ Eff* 38: 568–576.
14. Mašek O (2013) Production of biochar-different aspects of pyrolysis Biochar production, from lab to deployment; overview of challenges Pyrolysis/torrefaction and biochar production research at UKBRC.
15. Muvhiiwa R, Kuvarega A, Llana EM, et al. (2019) Study of biochar from pyrolysis and gasification of wood pellets in a nitrogen plasma reactor for design of biomass processes. *J Environ Chem Eng* 7: 103391.
16. Li F, Shen K, Long X, et al. (2016) Preparation and characterization of biochars from eichornia crassipes for cadmium removal in aqueous solutions. *PLoS One* 11: 7–9.
17. Joardder MUH, Halder PK, Rahim A, et al. (2014) Solar assisted fast pyrolysis: A novel approach of renewable energy production. *J Eng (United Kingdom)* 2014.
18. Flamant KG, Gauthier D, Guillot E (2015) Solar pyrolysis of wood in a Lab-scale solar reactor: Influence of temperature and sweep gas flow rate on products distribution. *Energy Procedia* 69: 1849–1858.
19. Soria J, Zeng K, Asensio D, et al. (2017) Comprehensive CFD modelling of solar fast pyrolysis of beech wood pellets. *Fuel Process Technol* 158: 226–237.
20. Matsunami J, Yoshida S, Yokota O, et al. (1999) Gasification of waste tyre and plastic (PET) by solar thermochemical process for solar energy utilization. *Sol Energy* 65: 21–23.
21. Sancho JA, María PA, José MT (2008) Catalytic air gasification of plastic waste (polypropylene) in fluidized bed. Part I: Use of in-gasifier bed additives. *Ind Eng Chem Res* 47: 1005–1010.
22. Albanese JAF, Ruiz MP (2015) Gasification of plastic waste as waste-to-energy or waste-to-syngas recovery route. *Apple Academic Press*: 267–290.
23. Joardder MUH, Halder PK, Rahim MA, et al. (2017) Solar pyrolysis: converting waste into asset using solar energy. *In Clean Energy for Sustainable Development, Academic Press*: 213–235.
24. Sharuddin SD, Faisal A, Daud WM, et al. (2016) A review on pyrolysis of plastic wastes. *Energy Convers Manage* 115: 308–326.
25. Hori T, Kobayashi K, Teranishi S, et al. (2020) Fuel cell and electrolyzer using plastic waste directly as fuel. *Waste Manage* 102: 30–39.
26. Duffie JA, Beckman WA, Blair N (2020) *Solar Engineering of Thermal Processes, Photovoltiacs and Wind, Jhon Wiley and Son, Inc. 5th Edition* .